Effect of welding parameters on properties of HDPE geomembrane seams

L. Zhang[1], A. Bouazza[2], R. K. Rowe[3] and J. Scheirs[4]

[1]PhD Student, Department of Civil Engineering, 23 College Walk, Monash University, Melbourne, Victoria 3800, Australia, E-mail: lu.zhang@monash.edu
[2]Professor, Department of Civil Engineering, 23 College Walk, Monash University, Melbourne, Victoria 3800, Australia, E-mail: malek.bouazza@monash.edu (corresponding author)
[3]Professor and Canada Research Chair in Geotechnical and Geoenvironmental Engineering, Department of Civil Engineering, Queen's University, Ellis Hall, Kingston, ON, Canada, K7L 3N6, E-mail: kerry.rowe@queensu.ca
[4]Principal Consultant, ExcelPlas Polymer Technology and Testing Services, 473 Warrigal Road, Moorabbin, Victoria 3189, Australia, E-mail: john@excelplas.com

Received 23 January 2017, revised 17 February 2017, accepted 20 February 2017

ABSTRACT: The effect of various welding parameters of a dual-wedge welding technique on the physical, mechanical and chemical properties of high-density polyethylene (HDPE) geomembrane seam specimens is examined. These seams were welded with sufficient heat, insufficient heat and excessive heat at specific speeds and nip pressures. The thickness of the fusion area and the width of the air channel provided an acceptable indication of the quality of the welding. Investigation of the seam specimens' mechanical properties showed that physical ageing had occurred. The impact of welding on antioxidants was evaluated using the standard oxidative induction time (Std-OIT) test method. The Std-OIT results showed that the outer edge of squeeze-out was greatly affected by the thermal welding. Scanning electron microscopy analysis confirmed that the morphology of the outer edge of squeeze-out was altered after welding. However, the Std-OIT test on other locations of the seam specimens indicated that welding had an insignificant impact on the Std-OIT values for the particular geomembrane and welding parameters considered.

KEYWORDS: Geosynthetics, Geomembrane, Seams, Welds, Temperature, Antioxidant depletion, Shear test, Peel test, MFI

REFERENCE: Zhang, L., Bouazza, A., Rowe, R. K. and Scheirs, J. (2017). Effect of welding parameters on properties of HDPE geomembrane seams. *Geosynthetics International*. [http://dx.doi.org/10.1680/jgein.17.00011]

1. INTRODUCTION

Geomembranes (GMBs) are flexible polymeric sheets mainly employed as liquid and/or vapour/gas barriers. They are designed as relatively impermeable liners and have been extensively used, over the past two decades, in lining barrier systems for waste containment facilities for a large spectrum of waste (Bouazza *et al*. 2002, 2014; Rowe 2005, 2012; Fourie *et al*. 2010; Hornsey *et al*. 2010; McWatters *et al*. 2016; Touze-Foltz *et al*. 2016). One of the key elements for a successfully functioning barrier system is the seaming (welding) in the field of the deployed GMB panels. GMBs are mostly welded by thermal methods, which rely on fusion of the surfaces to be joined using applied heat (i.e. wedge welding, hot air welding, and extrusion welding). Therefore, the quality of the GMB welds is significantly affected by welding temperature, welding speed, welding pressure and on-site conditions (particularly ambient temperature). These parameters have a major influence on the welds short-term behaviour (Scheirs 2009) and potentially their long-term behaviour (Shoaib and Rowe 2013; Rowe and Shoaib 2014). There are also a number of other factors that can lead to weld defects such as scoring along welds, thickness reduction on or near welds, adhered dirt or particulate contamination, notch effects and stress concentrations in or near welds, stress cracking, etc. (Scheirs 2009). All these factors have potential impacts on the long-term integrity of the welds.

Rollin *et al*. (1999) reported that 55% of the damage recorded in exposed GMB liners installed in basins, ponds and landfills occurred at seams. More recently, Gassner and Fairhead (2014) conducted a leakage rate survey on 67 liquid holding ponds, which mostly comprised

polyethylene liners with less than 7 m depth of stored liquid. The survey covered lined areas ranging from approximately 800 m^2 to 325 000 m^2. They reported that 32% of the defects recorded were defective seams, with most of them occurring on the floor of the ponds. They also reported that all the defects recorded on the slopes were related to faulty seams. Seams are the weakest points of a GMB and many problems (e.g. stress cracking) encountered in waste containment facilities and lined ponds originate at seam locations (Scheirs 2009; Peggs *et al.* 2014). Thermal welding temperature could normally be 3–4 times higher than the melting temperature of the GMB. The impact of the increased heat used in welding on seams is fraught with uncertainty, and there is a paucity of information in the literature comparing the material properties between GMB sheet sections and seam sections.

The objective of this paper is to investigate the effect of dual-hot wedge welding on high-density polyethylene (HDPE) GMB seams. This study is part of a larger programme investigating the durability of GMB seams under aggressive conditions at Monash and Queen's Universities. For this purpose, GMB specimens were welded with sufficient heat, insufficient heat and excessive heat. The impact of thermal welding on GMBs was evaluated from physical, mechanical and chemical aspects.

2. MATERIALS

The smooth HDPE GMB used in the present investigation is commonly used in pond/lagoon liners. The properties of the HDPE GMB are shown in Table 1 based on the tests conducted independently at Monash University. Three groups denoted as HS (hot and slow), S (standard) and CF (cool and fast) are reported in Table 1. They represent three lots of welded samples, all of which were from the same GMB roll and delivered to the Monash laboratory once the welding was completed by a specialised GMB installer. The supplier did not provide the technique used to manufacture the GMB. However, the high melt flow rate ratio (MFRR) reported in Table 1 suggests that the GMB was manufactured by the blown film method (Ewais and Rowe 2014).

2.1. Hot wedge welding

Three types of seams welded by dual-track wedge welding were assessed in this study. The welding was conducted using a Demtech XL welding machine. The machine had spring-loaded nip rollers to generate pressure on the heated polymer and create the weld. The compression spring pre-load was adjusted according to the sheet thickness being welded, and it is this pre-load that was adjusted to change the pressure. Seam S had the pre-load correctly set for the 2 mm sheet. Seam HS had the pre-load set to 4-clicks (average pressure) and seam CF had the pre-load set to 2-clicks (low pressure). All the welds were conducted indoors at an ambient temperature of 25°C.

A review of close to 90 dual-track wedge weld records of 2 mm thick HDPE GMB performed at various sites in the states of Queensland, Victoria and South Australia was conducted to identify typical temperatures and speed settings. There are many factors to consider when setting the welding temperature and speed, therefore these reviews have uncertainties. Nevertheless, the outcome of the review (Figure 1) indicated that 62% of the seams were welded with temperatures in the range of 430–440°C, which can be deemed as the most commonly used standard welding temperature range in these three Australian states. The mean welding speed corresponding to the above range of temperatures is 1.7 to 2.0 m/min (Figure 2). The insert in the figure indicates that the mean speed tends to increase exponentially as temperature increases. The welding parameters of the three seams used in the present investigation are shown in Table 2. Seam HS was welded with excessive heat (450°C) and low speed (1 m/min), and thus can be classified as a poor seam based on the data reported in Figures 1 and 2. Seam S was welded with a standard heat of 435°C and speed of 1.5 m/min, and can be classified as a standard seam. Seam CF was welded with low/insufficient heat (390°C) and high speed (2 m/min), and can be classified as a very poor seam.

The cross sections of the seams, together with their photos, are shown in Figure 3. The main feature that distinguishes the dual-track wedge seam from other welding methods is the presence of an air channel located between two parallel tracks. Scheirs (2009)

Table 1. HDPE GMB properties

Material properties	ASTM method	HS	S	CF	Unit
Thickness	ASTM D5199	1.99 ± 0.01	1.94 ± 0.04	2.04 ± 0.04	mm
Std-OIT	ASTM D3895	208 ± 4	211 ± 13	229 ± 12	min
HP-OIT	ASTM D5885	1143 ± 66	1142 ± 11	1172 ± 5	min
Crystallinity	ASTM E794	49 ± 2.7	45 ± 4.3	45 ± 3.6	%
Crystallinity	ASTM D3418	49 ± 2.3	44 ± 3.8	44 ± 3.3	%
Yield strength	ASTM D6693/D6693M	40 ± 2.3	39 ± 1.3	40 ± 2.0	kN/m
Yield strain	ASTM D6693/D6693M	16 ± 1.3	17 ± 0.8	17 ± 1.2	%
Break strength	ASTM D6693/D6693M	68 ± 9.8	65 ± 6.7	69 ± 5.8	kN/m
Break strain	ASTM D6693/D6693M	768 ± 88.7	806 ± 93	818 ± 73.2	%
LLMFI	ASTM D1238 (2.16 kg/190°C)	0.096 ± 0.004	0.096 ± 0.004	0.096 ± 0.004	g/10 min
HLMFI	ASTM D1238 (21.6 kg/190°C)	12.8 ± 0.4	12.8 ± 0.4	12.8 ± 0.4	g/10 min
MFRR	HLMFI/LLMFI	133	133	133	Ratio

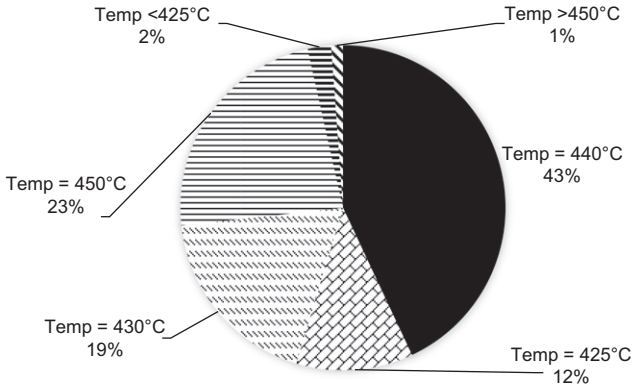

Figure 1. Welding temperature range of 2 mm HDPE GMBs at various sites in Australia

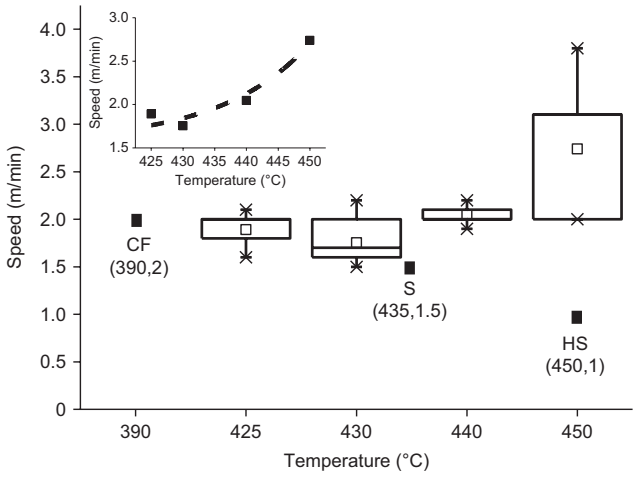

Figure 2. Relationship between welding temperature and speed. Note: the two diagonal crosses are the maximum and minimum values of the set of data. The crossbars at the ends of each whisker are the 95th and 5th percentile. The top and bottom boundaries of each box are the 75th and 25th percentile. The horizontal line inside each box is the median. The little square inside each box is the mean value. The welding temperature and speed of seams HS, S and CF are presented as a solid square in the graph

stated that the analysis of welds had demonstrated that there was a temperature gradient across the seam track. The mid-point of the seam track has the highest temperature, with the temperature decreasing to the two edges to a relatively low temperature. Hence, in the mid-region of the seam track, there is more molten material. As the heated-hot wedge melts the surfaces of the two overlapping HDPE GMB sheets, and the two melt layers are pressed together by the nip rollers immediately behind the wedges, it squeezes a small portion of the molten material out of the weld zone and forms what is referred to as 'squeeze-out' at each end of the seam track (Scheirs 2009).

3. RESULTS AND DISCUSSIONS

3.1. Dimensions and appearance identifications

Measurement of the thickness reduction of the finished seams can give a preliminary indication of their quality,

Table 2. Welding conditions

Welding condition	Welding temperature (°C)	Welding speed (m/min)	Welding start time	Welding finish time
Overheated [HS]	450	1	11:10	11:30
Standard [S]	435	1.5	12:00	12:13
Insufficient heat/ pressure [CF]	390	2	11:40	11:50

since the thickness reduction at the fusion area can have important implications with respect to the durability of the GMB. Generally, a thickness reduction implies less material per cross-sectional area to resist loads, but more importantly, the stress concentrations arising from an abrupt change in thickness is of particular concern (Scheirs 2009). In wedge welding, the fact that the centre of the weld track has more molten material, some of which is subsequently squeezed out laterally by nip pressure, can be assessed by measuring the thickness of the weld across its width. Generally, the centre of the weld is thinnest, and the thickness gradually increases towards each edge of the weld-track. Thus an important parameter for assessing the welding quality is the thickness reduction (T_r) at the fusion area. Thickness reduction is defined as the sum of the thicknesses of both top and bottom GMBs minus the seam track thickness (Scheirs 2009), viz

$$T_r = (T_t + T_b) \pm T_w \quad (1)$$

where T_r, is the thickness reduction; T_t, the thickness of the top GMB; T_b, the thickness of the bottom GMB and T_w, the thickness of the weld (or seam track).

Thickness measurements were conducted on the three types of seams. The thickness reductions of seams HS, S and CF are 1.22 mm, 0.66 mm and 0.23 mm respectively (Figure 4). Since seams HS, S and CF were welded at 450°C, 435°C and 390°C, it shows that as the welding temperature increased, the amount of thickness reduction increased for the welding speeds and nip pressures adopted. The thickness reduction of the weld can influence its long-term behaviour, particularly its toughness and water tightness (Scheirs 2009). Luders (2000) and Müller (2007) indicated that it is necessary to limit the extent of the thickness reduction to an acceptable range. According to the German guide (DVS 2225, from Scheirs 2009), the allowable seam thickness reduction for 1.5–2.0 mm thick HDPE GMBs should be within the range of 0.2–0.8 mm. Thus, based on the German guideline, it can be concluded that seam S is acceptable and Seam HS is not acceptable, whereas seam CF is borderline but acceptable. The above confirms the validity of the classification of the seams used in the present study.

Air channels are generally used to check the quality of the seam, and in this case air channel width provides an indication of the quality of the seam. As shown in Figure 5, the air channel widths of seams HS, S and CF are 4.33 mm, 6.83 mm and 12.33 mm, respectively. Through observation, seams welded at a higher temperature tend to have smaller air channels than seams welded at a lower temperature.

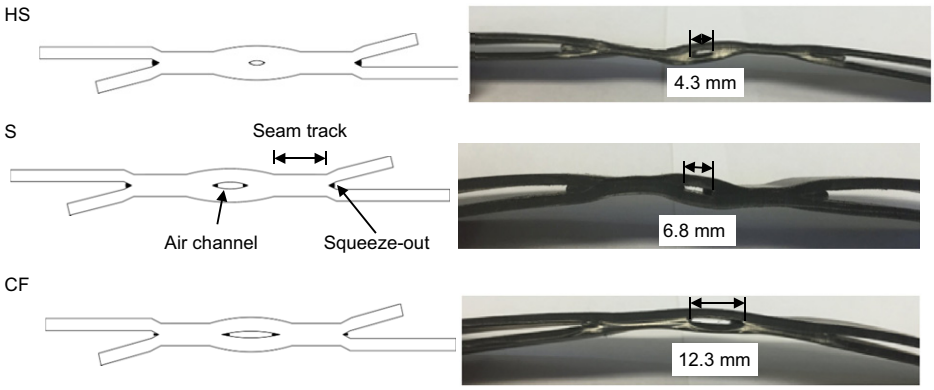

Figure 3. Schematic of the seam cross-sections (left); photos of the seam cross-sections (right). Sizes of air channels for seams HS, S and CF are presented (right). Note: photos are not to scale

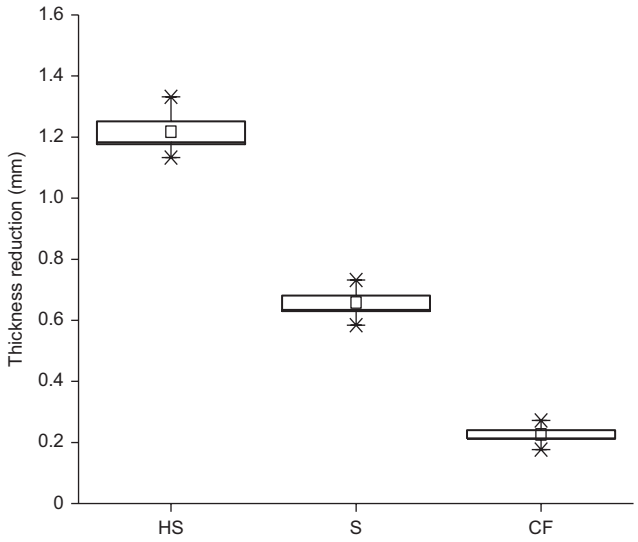

Figure 4. Thickness reduction of seam HS, S and CF. Note: sample size is 6 for each type of seam. The diagonal crosses are the maximum and minimum values of the set of data. The crossbars at the ends of each whisker are the 95th and 5th percentile. The top and bottom boundaries of each box are the 75th and 25th percentile. The horizontal line inside each box is the median. The small square inside each box is the mean value

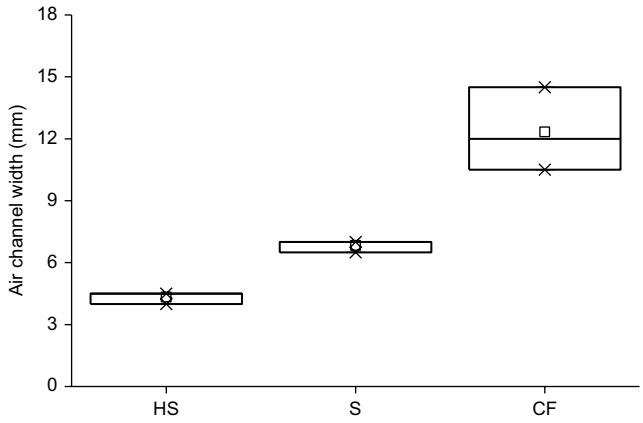

Figure 5. Air channel width of seams HS, S and CF. Note: sample size is 6 for each type of seam. The diagonal crosses are the maximum and minimum values of the set of data. The crossbars at the ends of each whisker are the 95th and 5th percentile. The top and bottom boundaries of each box are the 75th and 25th percentile. The horizontal line inside each box is the median. The small square inside each box is the mean value

There were no wave patterns observed in the direction of the weld due to the inherent stiffness of a thick (2 mm) GMB. However, the squeeze-out was noticed on both sides of the seam track. A small amount of squeeze-out usually means that a proper welding temperature has been achieved, as observed in seam S. Due to the excessive heat used in the welding process of seam HS, more molten polymer was squeezed out laterally to the sides of the nip rollers. Consequently, the sections adjacent to the seam HS track were thicker, and the thickness reduction of the weld was more severe. The size of the squeeze-out of seam HS was also larger than the other two seams, and it was an indication that excessive heat and pressure had been applied. It was observed that the squeeze-out was not uniform along the direction of seam CF. This was likely due to the fact that the welding temperature and pressure were not sufficient to produce enough molten polymer (i.e. there was less squeeze-out material). As a result, the size of the squeeze-out of seam CF was noticeably smaller compared to seams HS and S.

3.2. Mechanical properties

The mechanical properties of the seams were evaluated by conducting shear and peel tests in accordance with ASTM D6392. These two tests provide a decisive indication of the ductility and yield strength of the seams.

For the peel test, the specimens were fully gripped across their width. One grip clamped the upper layer and the other one clamped the bottom layer. A distance of 25 mm was secured on each side of the start of the seam bond. The test was conducted at a 50 mm/min loading rate, and terminated when the specimen ruptured. The peel test indicates if separation occurred within the weld region itself and confirms adequate bonding of the weld.

In this study, peel tests (ASTM D6392) were conducted 10 times on each type of seam, HS, S and CF. Figure 6 shows three examples of load-elongation curves related to

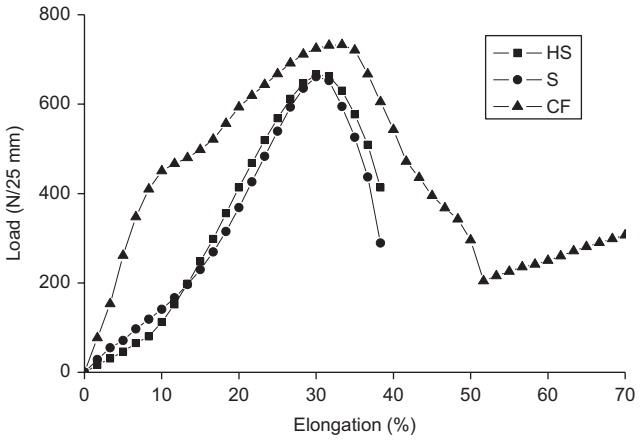

Figure 6. Load versus elongation for peel tests on welds conducted under three different conditions. The unit N/25 mm is compatible with GRI-GM19. The width of the test specimen is 25 mm. Note: seam separation only occurred on seam CF

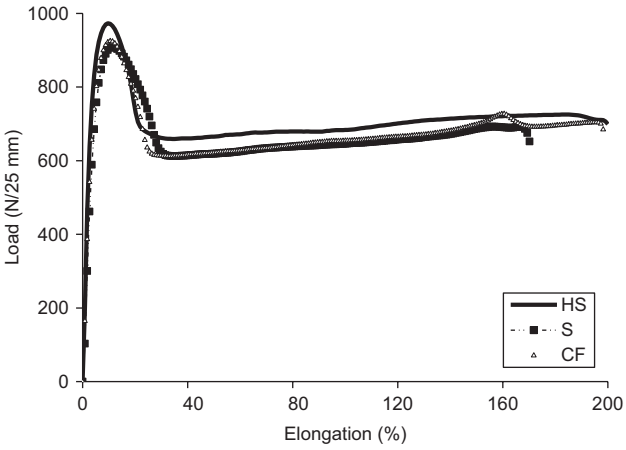

Figure 7. Load versus elongation for shears test on welds conducted under three different conditions. Note: the unit N/25 mm is compatible with GRI-GM19. The width of the test specimen is 25 mm

seam HS, S and CF from the peel tests. One can observe that seam HS and S share very similar behaviour; because proper welding parameters were achieved, as mentioned previously, no seam separation occurred. In contrast, bond separation was observed in seam CF and reflected in Figure 6. The load elongation curve of seam CF was distinctly different from seams HS and S. The area below the load-elongation curve of CF was larger than for seams HS and S. As this area represents the total energy consumed in a peel test, it indicates that more energy was required to pull the seam bond apart than to tear the GMB sheets (non-separated condition) apart. Up to 12% elongation, seam CF consumed about triple the energy expended on seams S and HS. After that, the peel strength of CF increased at a lower rate until it reached about 32% elongation, and then it gradually decreased.

The failure mode of seam CF was either AD-BRK (partial adhesion failure) or SE 1 (break in outer edge of seam). AD-BRK mode is an undesirable break code according to the ASTM D6392 'locus-of-break' codes, which classifies the various rupture modes of welds. Furthermore, two out of 10 specimens of seam CF had an exposed area of more than 25%. Since the maximum allowable separation area permitted by GRI-GM19 is less than 25%, seam CF failed GRI-GM19 (GRI 2015) as well. However, the peel strength of all the specimens was greater than the 530 N/25 mm required by GRI-GM19.

Shear elongation is very important for assessing the ductility of the welds as it can affect the longevity of the welds. The specimen was gripped across its full width, with a distance of 25 mm from each side of the start of the seam bond as per ASTM D6392. The shear test was conducted at 50 mm/min for seams HS, S and CF, and the results (Figure 7) show that they exhibited very similar mechanical behaviour in shear. They yielded at approximately 11%, and then a long plateau started at about 25% elongation. The break elongation for seams HS, S and CF is discussed later. No strain hardening was observed, and the yield and break strength of the three specimens were very similar for the three welds.

To identify the changes in mechanical properties after welding, a comparison of the load-extension behaviour between a virgin GMB and a seam specimen is shown in Figure 8. The load extension curve of the virgin GMB was obtained from tensile tests according to ASTM D6693/D6693M; whereas the load extension curve of the seam was obtained from shear tests according to ASTM D6392. Figure 8a shows the load-extension curve of a virgin GMB, and Figure 8b presents the load-extension curve of a seam specimen. There are four main differences between the results for these two specimens. First, the ultimate extension length of the virgin GMB (~400 mm) is about 1.3 times more than that for the seam (~270 mm). Second, strain hardening was only observed in the virgin GMB curve. Third, the ultimate strength (F_u) of the virgin GMB is higher than its yield strength (F_y), whereas the opposite was observed in the seam specimens. Fourth, the ultimate strength (F_u)

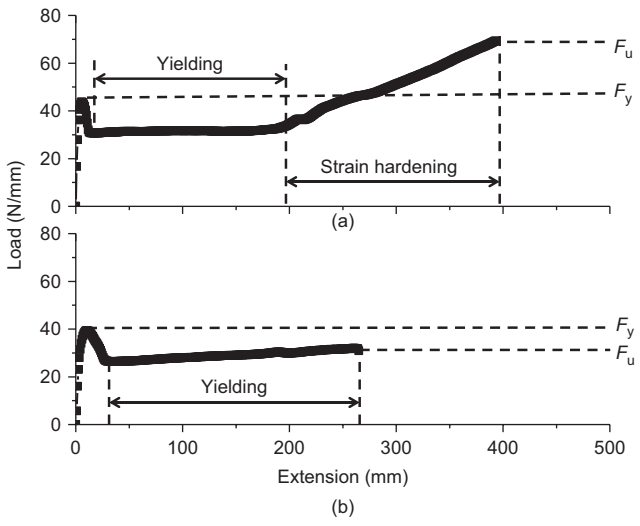

Figure 8. Comparison of the load-extension curve between (a) virgin GMB, and (b) seam S

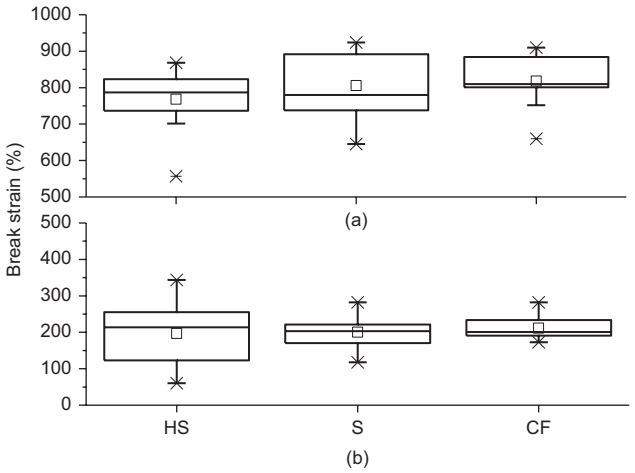

Figure 9. (a) Break strain of virgin GMBs (on specimens sampled away from the seam track section for each seam condition). (b) Break strain of seam specimens. Note: sample size is 10 for each type of seam. The diagonal crosses are the maximum and minimum values of the set of data. The crossbars at the ends of each whisker are the 95th and 5th percentile. The top and bottom boundaries of each box are the 75th and 25th percentile. The horizontal line inside each box is the median. The small square inside each box is the mean value

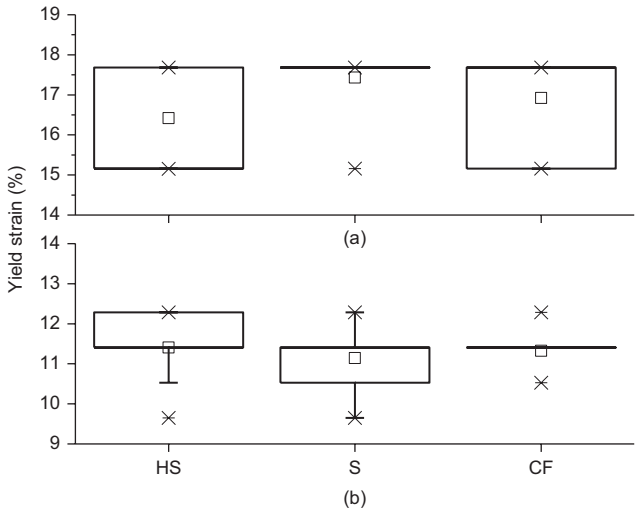

Figure 10. (a) Yield strain of virgin GMB (on specimens sampled away from the seam track section for each seam condition). (b) Yield strain of seam specimens. Note: sample size is 10 for each type of seam. The diagonal crosses are the maximum and minimum values of the set of data. The crossbars at the ends of each whisker are the 95th and 5th percentile. The top and bottom boundaries of each box are the 75th and 25th percentile. The horizontal line inside each box is the median. The small square inside each box is the mean value

of the virgin GMB is higher than the ultimate strength (F_u) of the seam specimens.

The impact of the wedge welding on the break strain of the seam specimens is shown in Figure 9. A total of 30 seam specimens (according to ASTM D6392) were sampled and tested. Furthermore, 20 specimens sampled from the virgin side of the GMB (i.e. away from the seam track section and referred to here as virgin GMB) for each seam condition were tested according to ASTM D6693/D6693M. The results show that approximately 50% of the virgin GMBs had break strains ranging from 750–850%, and the average break strain was approximately 800%. About 50% of seam HS specimens had break strains ranging from 120 to 250%, and approximately 50% of the seams of S and CF specimens had break strains ranging from 160 to 230%. Even though the range of the break strains of seam HS specimens was wider than either seam S or CF specimens, the medium and the mean of the three types of seams were all around 200%. Since the break strains of the seam specimens were all significantly lower than the virgin GMBs, one can conclude that welding can decrease the break strain of seam specimens and have a negative impact on the ductility of GMBs.

Similarly to the conditions for break strains, the yield strains of the seam specimens were also significantly smaller than the yield strains of the virgin GMB. The yield strains of seams HS, S and CF ranged from approximately 10% to 12%, while that of the virgin GMB ranged from approximately 15% to 18% (Figure 10). The average yield strains were 11% and 17% for the seam and virgin GMB specimens, respectively. Therefore, the welding technique employed here reduced the yield strain of the seam specimens by approximately 55% from their virgin status.

Despite the fact that the wedge welding technique reduced the break strains and the yield strains of the seam specimens; it had little impact on the yield strengths of the seam specimens. The yield strengths of the seam specimens ranged from approximately 35 kN/m to 39 kN/m, with an average of about 37 kN/m; and the yield strength of the virgin GMB ranged from approximately 38 kN/m to 41 kN/m, with an average of about 40 kN/m (Figure 11). To examine the statistical significance of the changes in the yield strength of the specimens, Student's t-test was conducted. The test results showed a 95% confidence level, thus there was insignificant difference between the yield strength of the seam specimens and the yield strength of the virgin GMB.

3.3. Melt flow index (MFI)

The melt flow index (MFI) test (ASTM D1238) is considered an indirect but convenient index, providing some insight into the molecular weight of polymers. Physical ageing and oxidative degradation can alter a GMB's molecular weight (Hsuan and Koerner 1998). To assess the impact of welding temperature on the seam specimens, MFI tests were conducted on both the virgin GMBs and the fusion area (or seam track) of seams HS, S and CF. Seam tracks were selected because they are in direct contact with the hot wedge during the welding process. Table 3 summarises the MFI results obtained from the virgin GMBs and the seam tracks. The modest changes noted suggest that there was no chemical degradation caused by the welding process.

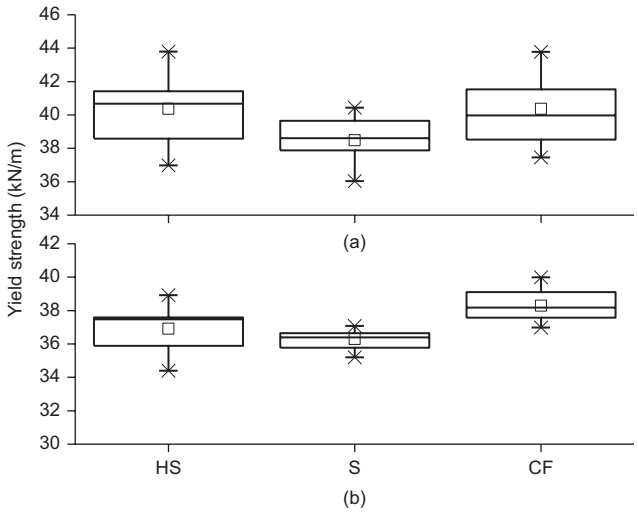

Figure 11. (a) Yield strength of virgin GMBs (on specimens sampled away from the seam track section for each seam condition). (b) Yield strength of seam specimens.
Note: Sample size is 10 for each type of seam. The diagonal crosses are the maximum and minimum values of the set of data. The crossbars at the ends of each whisker are the 95th and 5th percentile. The top and bottom boundaries of each box are the 75th and 25th percentile. The horizontal line inside each box is the median. The small square inside each box is the mean value

3.4. Standard oxidative induction time (Std-OIT)

The Std-OIT test is a standardised method (ASTM D3895) commonly used to assess the quantity of antioxidants present in a GMB. It is defined as the period of time between the first exposure to oxygen and the onset to oxidation. The test terminates when the exothermic peak appears. The onset of an exothermic reaction of the polymer with oxygen is signalled by the transition to the steep slope in the thermogram shown in Figure 12. In the current study, the Std-OIT test was used to assess the impact of welding on the oxidation resistance of seams HS, S and CF by testing the quantity of antioxidants retained in the seam specimens at different locations after welding.

Five specific locations (Figure 13) on each type of seam specimen were selected to evaluate the impact of welding. Location 1 was a non-structural sampling location situated at the outer edge of the squeeze-out (the edge facing away from the seam track). Location 2 (the heat affected zone) was on the sheet (either top or bottom) adjacent to the seam track. Location 3 was the virgin GMB, which was unaffected by the welding and away from the heat affected zone. Location 7 was on the weld (seam track) where the two pieces of GMBs were fused into one as a whole, and Location 8 was the GMB located either above or below the air channel. Locations 1, 2, 7 and 8 were selected because they were in close contact with the hot wedge during the welding process. Location 3 was used as a reference value for the purpose of comparative analysis, since it was unaffected by the welding. Each Std-OIT test specimen was taken across the whole thickness and was 1.5 ± 0.4 mm wide.

The Std-OIT test was conducted on three or more replicates for each selected location. The average results and standard deviations of locations 2, 3, 7 and 8 are shown in Table 4. They had similar Std-OIT values, ranging from approximately 200 min to 220 min, and their standard deviations were all within 10 min. A statistical analysis was conducted to assess the changes in the Std-OIT value after welding by comparing the Std-OIT values of Locations 2, 7 and 8 with the reference value of Location 3. As shown in Table 5, the Std-OIT values at Location 2 for seam HS, S, and CF decreased by 7%, 4% and 7%, respectively. Even though Location 2 is prone to stress cracking (Peggs *et al.* 2014), the slight difference in the Std-OIT values between Location 2 and Location 3 shows that the welding temperature, speed and pressure had a negligible impact on the oxidation resistance of the seam specimens for the specific GMB and welding conditions examined. A similar trend was also observed from Location 7 and 8. The Std-OIT values at Location 7 for seams HS, S, and CF decreased by 3%, 1% and 8%, and the Std-OIT values at Location 8 for seam HS, S, and CF decreased by 3%, 0% and 8%, respectively. The above results indicate that welding had an insignificant impact on the oxidation resistance of the seam specimens. Furthermore, the retained Std-OIT values were found to all be above the minimal values required by GRI-GM13 (GRI 2016) for all the seam types.

Unlike Locations 2, 7, and 8, Location 1 (the edge of the squeeze-out) did not retain a Std-OIT value as high as 200 min, and abnormal thermograms were observed for Location 1 specimens (e.g. Figures 14a and 14b). A conventional Std-OIT thermogram has a uniform heat flow after the purged gas is switched to oxygen at 200°C until an exothermic reaction occurs (an exothermic peak in the diagram; Figure 12). Conventional Std-OIT thermograms were observed in Locations 2, 3, 7 and 8, whereas the thermograms obtained from the specimens at Location 1 showed a non-uniform heat flow after the purged gas was switched to oxygen at 200°C, and multiple

Table 3. MFI results: comparison between virgin GMB sheet and seam track section

Seam	Virgin	HS	S	CF
Section	Sheet	Seam track	Seam track	Seam track
LLMFI (g/10 min)	0.096 ± 0.004	0.089 ± 0.002	0.096 ± 0.003	0.101 ± 0.003
HLMFI (g/10 min)	12.8 ± 0.4	12.0 ± 0.3	12.7 ± 0.2	12.5 ± 0.3
MFRR (HLMFI/LLMFI)	133	135	131	123

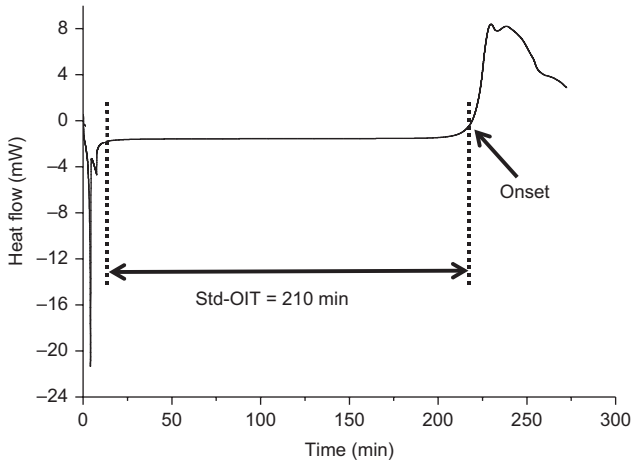

Figure 12. Thermogram of the conventional Std-OIT
Note: uniform heat flow is shown on the curve. The onset is shown on the conventional Std-OIT curve

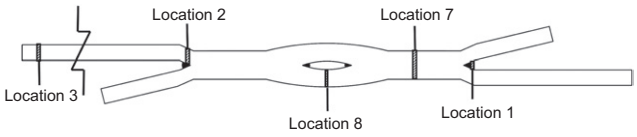

Figure 13. Schematic cross-section view, which shows the sampling locations of the Std-OIT test and the crystallinity test sampling locations of a seam specimen

Table 4. Std-OIT test results of Location 2, 3, 7 and 8 (mean ±standard deviation based on minimum of three tests)

Location	HS (min)	S (min)	CF (min)
2	196 ± 11	207 ± 2	209 ± 2
3	208 ± 4	211 ± 13	220 ± 20
7	207 ± 1	220 ± 3	207 ± 1
8	208 ± 1	223 ± 15	206 ± 1

onsets were observed before the exothermic peak appeared. In addition, it should be noted that the Std-OIT test results of the seam specimens collected from Location 1 were not replicable. The non-uniform heat flow masked the true onset of the exothermic reaction. For instance, Figure 14a shows that two different OIT values were yielded from the same thermogram. The time lag between the two onsets was about 100 min. The first onset yielded a Std-OIT value of 18 min, and the second onset yielded a Std-OIT value of 120 min. Since multiple onsets can be drawn from the same thermogram, the Std-OIT test results at Location 1 have broad ranges of values. The Std-OIT range for seams HS, S and CF were 10–190 min, 9–220 min and 190–200 min, respectively.

The most likely reason for the observed multiple peaks in the Std-OIT curve (Figure 14) is the occurrence of multiple oxidative transitions that arise from sample inhomogeneity. This has been reported previously by Scheirs (2000). The root cause of the multiple oxidative transitions is sample inhomogeneity that occurs when polyethylene is quickly oxidised on the surface where there is full contact with oxygen and negligible oxidation under the surface of the sample due to hindered oxygen diffusion, as would occur on the squeeze-out bead. This leads to a significant disparity in residual antioxidant levels. In addition due to the rapid surface cooling and slow cooling of the inside of the squeeze-out bead, a pronounced crystallisation gradient occurs across the squeeze-out bead leading to the so-called 'skin-core' morphology that leads to sample inhomogeneity.

3.5. Scanning electron microscopy (SEM) analysis

SEM (a Nova NanoSEM 450 at 2 kV) was used to investigate the impact of welding on the squeeze-out. A double-sided sticky carbon tape was placed between the specimens and the metal stud to fix the specimens. The carbon tape was also wrapped around the specimen and the stud to create a physical medium, allowing electrons to interact with the non-conductive HDPE seam specimens without damaging the specimens during the test.

Figures 15a and 15b show that the squeeze-out of seam S has two distinguishable surfaces that can be identified as the smooth surface and the rough surface. Figure 15a shows the rough surface, which is close to the seam track and Figure 15b shows the surface of the outer edge. Both surfaces are presented in Figure 15b and are separated by a dotted line. The images show that welding had different impacts on the squeeze-out.

The 5000× magnification view (Figure 16) of the squeeze-out close to the seam track shows that the roughness was actually surface distortion. The bright lines on the surface are signs of surface distortion. The more bright lines that are present in a specific area, the higher the degree of surface distortion. The dark area means there is little or no distortion.

Figure 17 presents the 5000× magnification view of the external edge of the squeeze-out. Under 5000× magnification, the smooth surface is shown to be fibre-like. Under

Table 5. Average Std-OIT value of Locations 2, 7, 8 relative to that at Location 3

Location	HS		S		CF	
2	−14 min	−7%	−9 min	−4%	−16 min	−7%
7	−6 min	−3%	−2 min	−1%	−17 min	−8%
8	−5 min	−3%	1 min	0%	−18 min	−8%

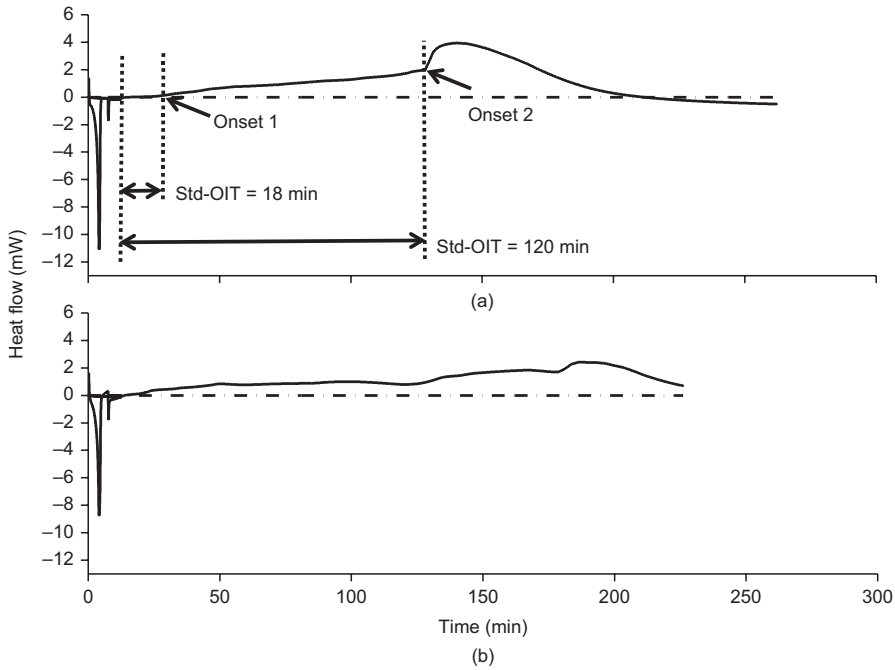

Figure 14. Thermograms of Std-OITs at Location 1. Note: non-uniform heat flow is shown on the curve. The onsets of the exothermic reaction of (a) and (b) are not clear

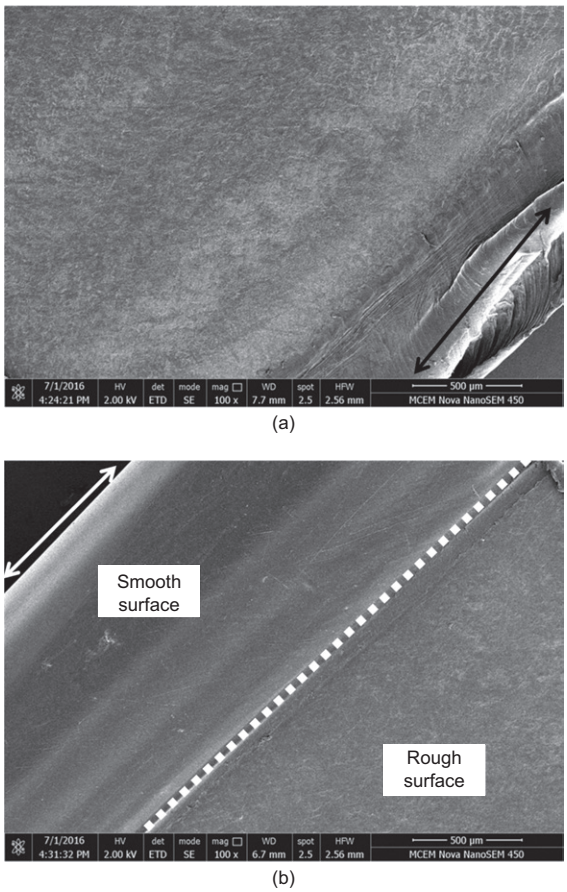

Figure 15. SEM with 100× magnification of the surface of the squeeze-out of seam S. Note: the inner edge of the squeeze-out (a) adjacent to the seam track and the outer edge of the squeeze-out (b) away from the seam track are indicated by the double-headed arrows. In (b), the smooth surface and rough surface are separated by the dotted line

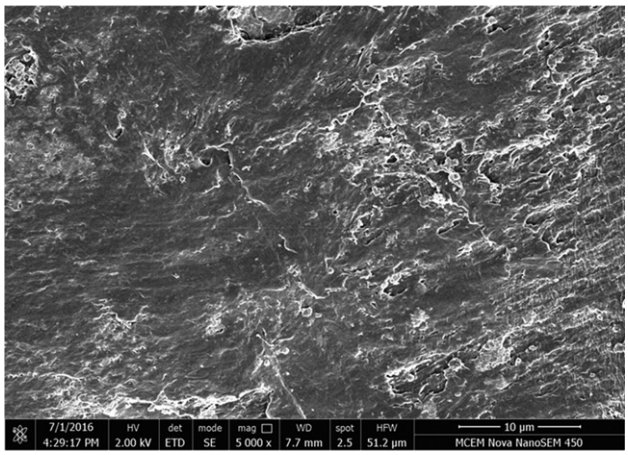

Figure 16. SEM with 5000× magnification of the surface of the squeeze-out of seam S. Images were taken from the inner edge, which was close to the seam track

the same magnification, the surface of the virgin GMB is relatively smooth and intact (Figure 18). The differences in the surface appearance after welding indicate that the thermal welding altered the polymer morphology of the squeeze-out. Monitoring the change in morphology of the squeeze-out is important in understanding its thermal history and the uniformity of welding, in particular the nip pressure uniformity and spatial temperature uniformity. The change of the morphology observed here indicates that non-uniform heating and/or non-uniform nip pressure have taken place, and explains why non-uniform heat flow was only obtained in Location 1. It also indicates that the explanation for the non-uniform thermogram suggested above is highly likely.

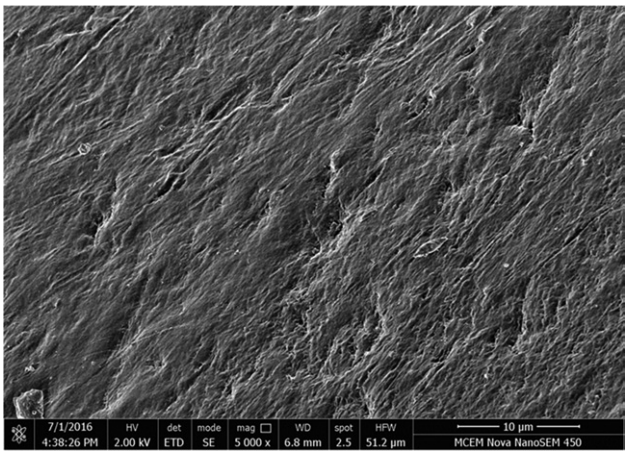

Figure 17. SEM with 5000× magnification of the surface of the squeeze-out of seam S. Images were taken from the outer edge, away from the seam track

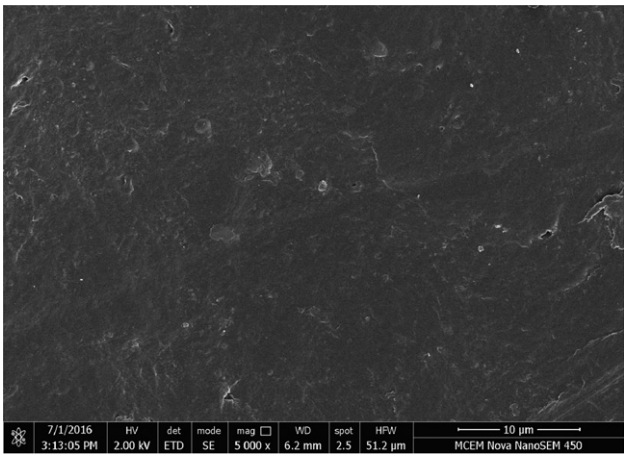

Figure 18. SEM with 5000× magnification of the surface of the virgin GMB

4. CONCLUSIONS

The study investigated the effect of welding on HDPE GMB seam sections welded using sufficient heat (S), insufficient heat (CF) and excessive heat (HS). For the specific GMB and conditions examined, the following conclusions can be drawn from this study

(1) Monitoring of the thickness reduction and air channel width can give a preliminary indication of the quality of the finished seams and amount of squeeze-out. Recommendations for (a) acceptable ranges of thickness reduction for different initial sheet thicknesses being welded, (b) air channel size, and (c) the proper amount of squeeze-out can be given against a reference standard such as a trial seam made under ideal standard conditions.
(2) The mechanical properties of the seams were all significantly weaker than those of the virgin GMB. This was due to the abrupt change of shape when two independent GMBs were welded into one piece.
(3) Peel tests indicated that separation occurred in 20% of seam CF.
(4) Dual wedge welding had an insignificant impact on the Std-OIT of the seam specimens, except for at Location 1. Furthermore, the retained Std-OIT values were found to be above the minimal values required by GRI-GM13 for all the seam types.
(5) The Std-OIT test shows that the outer edge of the squeeze-out (Location 1) was affected by the welding.
(6) The observation of multiple peaks in the Std-OIT curves of the squeeze-out beads can be attributed to multiple oxidative transitions arising from sample inhomogeneity, both from an antioxidant distribution perspective due to non-uniform antioxidant consumption and from a morphological perspective due to non-uniform sample cooling.
(7) SEM analysis shows that the polymer morphology of the squeeze-out was altered by the thermal welding, confirming the reasons for the occurrence of the multiple peaks in the Std-OIT curves.

ACKNOWLEDGEMENT

The authors are very grateful to G. Fairhead (FABTECH) for supplying the geomembrane seam samples used in this study.

NOTATION

Basic SI units are given in parentheses.

F_u ultimate strength (N/m)
F_y yield strength (N/m)
T_b thickness of the bottom GMB (m)
T_r thickness reduction (m)
T_t thickness of the top GMB (m)
T_w thickness of the weld (m)

ABBREVIATIONS

GMB	Geomembrane
GRI	Geosynthetic research institute
HDPE	High-density polyethylene
HLMFI	High load melt flow index
HP-OIT	High pressure oxidative induction time
LLMFI	Low load melt flow index
MFI	Melt flow index
MFRR	Melt flow rate ratio
SEM	Scanning electron microscopy
Std-OIT	Standard oxidative induction time

REFERENCES

ASTM D6693/D6693M-04 *Standard Test Method for Determining Tensile Properties of Nonreinforced Polyethylene and Nonreinforced Flexible Polypropylene Geomembranes.* ASTM International, West Conshohocken, PA, USA.

ASTM D5199-12 *Standard Test Method for Measuring the Nominal Thickness of Geosynthetics*. ASTM International, West Conshohocken, PA, USA.

ASTM D6392-12 *Standard Test Method for Determining the Integrity of Non-Reinforced Geomembrane Seams Produced Using Thermo-Fusion Methods*. ASTM International, West Conshohocken, PA, USA.

ASTM D1238-13 *Standard Test Method for Melt Flow Rates of Thermoplastics by Extrusion Plastometer*. ASTM International, West Conshohocken, PA, USA.

ASTM D3895-14 *Standard Test Method for Oxidative-Induction Time of Polyolefins by Differential Scanning Calorimetry*. ASTM International, West Consohocken, PA, USA.

ASTM D3418-15 *Standard Test Method for Transition Temperatures and Enthalpies of Fusion and Crystallization of Polymers by Differential Scanning Calorimetry*. ASTM International, West Consohocken, PA, USA.

ASTM D5885-15 *Standard Test Method for Oxidative Induction Time of Polyolefin Geosynthetics by High-Pressure Differental Scanning Calorimetry*. ASTM International, West Consohocken, PA, USA.

ASTM E794-06 *Standard Test Method for Melting And Crystallization Temperatures by Thermal Analysis*. ASTM International, West Consohocken, PA, USA.

Bouazza, A., Zornberg, J. & Adam, D. (2002). Geosynthetics in waste containments: recent advances. *Proceedings 7th International Conference on Geosynthetics*, Nice, France, Balkema, Lisse, The Netherlands, vol. 2, pp. 445–507.

Bouazza, A., Singh, R. M., Rowe, R. K. & Gassner, F. (2014). Heat and moisture migration in a geomembrane-GCL composite liner subjected to high temperatures and low vertical stresses. *Geotextiles and Geomembranes*, **42**, No. 5, 555–563.

Ewais, A. M. R. & Rowe, R. K. (2014). Effects of blown film process on initial properties of HPDE geomembranes of different thicknesses. *Geosynthetics International*, **21**, No. 1, 62–82.

Fourie, A., Bouazza, A., Lupo, J. & Abrao, P. (2010). Improving the performance of mining infrastructure through the judicious use of geosynthetics. *Proceedings 9th International Conference on Geosynthetics*, Sao-Paulo, Brazil, IGS-Brazil, Sao Paulo, Brazil, pp. 193–218.

Gassner, F. & Fairhead, G. (2014). Field leakage rates of geosynthetic lined facilities. *Proceedings 10th International Geosynthetics Conference*, Berlin, Germany, DGGT, Essen, Germany (CD-ROM).

GRI (Geosynthetic Research Institute) (2015). *GRI Test Method GM19. Seam Strength and Related Properties of Thermally Bonded Polyolefin Geomembranes*, Geosynthetic Institute, Philadelphia, PA, USA.

GRI (2016). *GRI GM 13 Test Methods. Test Properties and Testing Frequency for High Density Polyethylene (HDPE) Smooth and Textured Geomembranes*, Geosynthetic Institute, Philadelphia, PA, USA.

Hornsey, W. P., Scheirs, J., Gates, W. P. & Bouazza, A. (2010). The impact of mining solutions/liquors on geosynthetics. *Geotextiles and Geomembranes*, **28**, No. 2, 191–198.

Hsuan, Y. & Koerner, R. (1998). Antioxidant depletion lifetime in high density polyethylene geomembranes. *Journal of Geotechnical and Geoenvironmental Engineering*, **124**, No. 6, 532–541.

Luders, G. (2000). Quality assurance in hot wedge welding of HDPE geomembranes. *Proceedings 2nd European Geosynthetics Conference*, Bologna, Italy, Patron Editore, Bologna, Italy, vol. 2, pp. 591–596.

McWatters, R. S., Rowe, R. K., Wilkins, D., Spedding, T., Jones, D., Wise, L., Mets, J., Terry, D., Hince, G., Gates, W. P., Di Battista, V., Shoaib, M., Bouazza, A. & Snape, I. (2016). Geosynthetics in Antarctica: performance of a composite barrier system to contain hydrocarbon-contaminated soil after three years in the field. *Geotextiles and Geomembranes*, **44**, No. 5, 673–685.

Müller, W. (2007). *Welding of HDPE Geomembranes. HDPE Geomembranes in Geotechnics*, Springer Berlin Heidelberg, Berlin, Heidelberg, Germany, pp. 379–420.

Peggs, I. D., Gassner, F., Scheirs, J., Tan, D., Arango, A. M. N. & Burkard, B. (2014). Is there a resurgence of stress cracking in HDPE geomembranes? *Proceedings 10th International Geosynthetics Conference*, Berlin, Germany, DGGT, Essen, Germany (CD-ROM).

Rollin, A. L., Marcotte, M., Jacqueline, T. & Chaput, L. (1999). Leak location in exposed geomembrane liners using an electrical leak detection technique. *Proceedings of Geosynthetic'99, Industrial Fabrics Association International*, Boston, USA, IFAI, Roseville, MI, USA, vol. 2, pp. 615–626.

Rowe, R. K. (2005). Long-term performance of contaminant barrier systems; The 45th Rankine Lecture. *Geotechnique*, **55**, No. 9, 631–678.

Rowe, R. K. (2012). Short and long-term leakage through composite liners; The 7th Arthur Casagrande Lecture. *Canadian Geotechnical Journal*, **49**, No. 2, 141–169.

Rowe, R. K. & Shoaib, M. (2014). Effect of brine on STD-OIT depletion from HDPE GMB seams. *Proceedings 7th International Congress on Environmental Geotechnics*, Melbourne, Engineers Australia, Canberra, Australia, pp. 472–479.

Scheirs, J. (2000). *Compositional and Failure Analysis of Polymers: A Practical Approach*, John Wiley & Sons Ltd., Chichester, UK.

Scheirs, J. (2009). *A Guide to Polymeric Geomembranes: A Practical Approach*, John Wiley & Sons Ltd., Chichester, UK.

Shoaib, M. & Rowe, R. K. (2013). Durability and long-term strength of seams in HDPE geomembranes. *Proceedings 66th Canadian Geotechnical Conference*, Montreal, CGS, Richmond, Canada, paper 342.

Touze-Foltz, N., Bannour, H., Barral, C. & Stoltz, G. (2016). A review of the performance of geosynthetics for environmental protection. *Geotextiles and Geomembranes*, **44**, No. 5, 656–672.

The Editor welcomes discussion on all papers published in Geosynthetics International. Please email your contribution to discussion@geosynthetics-international.com